Identifying Autism Spectrum Disorder with Multi-Site fMRI via Low-Rank Domain Adaptation – *Supplementary Materials*

Mingliang Wang, Daoqiang Zhang*, Jiashuang Huang, Pew-Thian Yap, Dinggang Shen*, *Fellow, IEEE*, Mingxia Liu*, *Senior Member, IEEE*

In what follows, we first report additional experimental results achieved by the proposed multi-site adaptation based on low-rank representation (maLRR) method and competing methods on a labeled synthetic dataset. We then present the results of different methods for Autism Spectrum Disorder (ASD) diagnosis on the whole Autism Brain Imaging Data Exchange (ABIDE) database [1], [2], with functional MRI data pre-processed by using both the Anatomical Automatic Labeling (AAL) atlas [3] and the CC200 atlas [4]. We also evaluate the proposed method on unbalanced multi-site autism spectrum disorder (ASD) dataset and analyze the brain connectivity patterns identified by our method. In addition, we analyze the convergence of the proposed optimization algorithm for solving the proposed maLRR model and present the details of the proposed optimization algorithm.

A. Results on Labeled Synthetic Data

As mentioned in the main text, we use a toy example with unlabeled synthetic data to show the effectiveness of our maLRR method in reducing the difference of domain distributions. Here, we further perform a group of experiments on a labeled synthetic dataset to evaluate the homogeneity of the data after adaptation using our maLRR method. Specifically, as shown in Fig. S1 (a), we generate three sets/domains of samples, with each set represented by a specific color. Here, we treat the domain marked as blue as the target domain, while those marked as red and green as two source domains. In each domain, there are 100 labeled samples from one category (*e.g.*, denoted as circles) and 100 labeled samples from another category (*e.g.*, denoted as triangles).

1) Data Visualization Before and After Adaptation: We first visually show the data distributions of our synthesized labeled dataset using both our maLRR method and the Robust Domain Adaptation via Low-rank Reconstruction (RDALR) method [5]. Different from our maLRR that simultaneously transforms both source and target domains to a common latent space, the RDALR method simply transforms multi-source data to the target domain. For the original data shown in Fig. S1 (a), we can obtain new representations for all samples in three domains using our maLRR method and the RDALR method, respectively. The new representations after data adaptation are shown in Fig. S1 (b) and Fig. S1 (c), from which we can see that our maLRR method can transform data from three domains into a more compact region.

2) Classification Results: To evaluate the data homogeneity before and after adaptation, we further perform a classification experiment using the original and new data representations of the labeled synthetic data. We compare our maLRR with the following methods: (1) Baseline-1 that uses the original features, (2) low-rank representation (LRR) [6], (3) RDAL-R [5], transfer component analysis (TCA) [7], (4) denoising autoencoder (DAE) [8], and (5) the variant of our method (*i.e.*, maLRR-1) that simply transforms source domains to the target domain (see Eq. 4 in the main text).

Specifically, for the Baseline-1 method, we learn an SVM classifier with the polynomial kernel (default parameters) based on the original features of samples from two source domains, and then apply this classifier to the samples in the target domain for binary classification. Since representation-based methods (*i.e.*, LRR, RDALR, TCA, maLRR-1, and maLRR) can only learn new representations for samples in multiple domains, we also employ the SVM with the polynomial kernel (default parameters) as classifier based on the learned representations for classification. Two hidden layers in the DAE method [8] for the encoder and decoder contain 64 and 32 units, respectively.

Using the original feature representation, Baseline-1 obtains an accuracy of 93.50% for the identification task in the target domain. With the new representations after data adaptation via the representation-based methods (i.e., LRR, RDALR, TCA, DAE, maLRR-1, and maLRR), the classification accuracies for the target samples are 75.50%, 89.00%, 85.50%, 71.50%, 83.00% and 96.00%, respectively. One can observe that our maLRR consistently outperforms the competing methods using the original/new data representations, suggesting its effec-

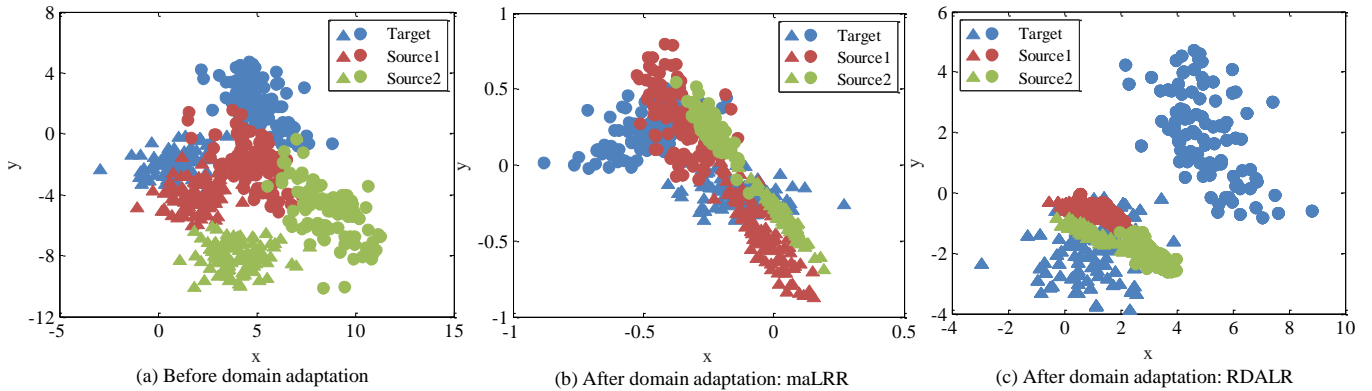(a) Before domain adaptation   (b) After domain adaptation: maLRR   (c) After domain adaptation: RDALR

Fig. S1. Results on labeled synthetic data achieved by our maLRR and RDALR methods, with the same color denoting the same domain and the same shape representing the same category. Here, samples represented by blue are treated as the to-be-analyzed target domain, while samples in green and red are treated as source domains. (a) Data distributions of three domains in the original space. (b) Data distributions in the common space after transformation via our maLRR method. (c) Data distributions in the common (*i.e.*, target) space after transformation via the RDALR method (transforming source data to the target domain).

tiveness of transforming the original multi-domain data into a common space to reduce the difference in data distributions. Also, our method yields better performance than the RDALR method that simply transforms multi-source data to the target domain, suggesting the effectiveness of the proposed 2nd strategy (*i.e.*, further linearly representing source data using target data in the common latent space).

B. Results on Whole ABIDE Database

As mentioned in the main text, considering that several sites contain only a limited number of participants, we just use the data (pre-processed using the AAL atlas) from 5 imaging sites (*i.e.*, *NYU*, *Leuven*, *UCLA*, *UM*, and *USM*) in the ABIDE cohort. Here, we have now added a new group of experiments on the whole ABIDE cohort with fMRI data from all imaging sites [1], [2], and also pre-processed these fMRI data using both the AAL atlas [3] and the CC200 atlas [4]. In Table SI, we show the detailed demographic information of subjects from all 17 imaging sites in ABIDE. Note that we do not use the *CMU* site because there is only one subject in this imaging site. All fMRI data are pre-processed by using the Configurable Pipeline for the Analysis of Connectomes (C-PAC) [9], and the pre-processed data from 16 imaging sites are downloaded online[1]. Thus, we have a total of 801 subjects (with 432 ASD patients and 369 NCs) and 830 subjects (with 446 ASD patients and 384 NCs) pre-processed using the AAL atlas and CC200 atlas, respectively.

In this group of experiments, we compare our maLRR method with five competing methods, including Baseline-1, LRR, TCA, DAE, and maLRR-1. We treat each site as the to-be-analyzed target domain in turn, and the remaining 15 sites as the source domains. For the Baseline-1 method, we directly train a linear SVM model (with the default penalty parameter) on the combined subjects from multiple source domains, and apply the trained model to subjects in the target domain. For four representation-based methods (*i.e.*, LRR, TCA, maLRR-1 and maLRR), we first learn new representations for both source data and target data using a specific algorithm, and then

[1] http://preprocessed-connectomes-project.org/abide/

feed the learned representation to a linear SVM (with the default penalty parameter) for ASD identification. The parameter settings for Baseline-1, LRR, TCA, maLRR-1 and maLRR are the same as described in the last paragraph of Section IV-B in the main text. As an end-to-end learning method, the DAE method [8] shares the same input as our method (see Section IV-A-2 in the main text) for the fair comparison. Besides, the DAE model employs the same architecture as [8] when using the CC200 atlas. When using the AAL atlas, two hidden layers in DAE have 800 and 400 units, respectively. Due to the limited number of participants in the *SBL* site (*i.e.*, < 10, pre-processed by the AAL atlas), we employ a 2-fold cross-validation strategy to evaluate the performance of all methods. The experimental results on the whole ABIDE database using the AAL atlas and the CC200 atlas are shown in Table SIII and Table SIV, respectively.

From Tables SIII-SIV, one may have the following observations. *First*, our maLRR method generally achieves better performance, compared with the competing methods using both the AAL and CC200 atlases on 16 imaging sites. These results further validate the efficacy of our proposed method for multi-site disease identification. *Second*, the overall classification results achieved by our maLRR method using 16 imaging sites are slightly lower than those yielded by maLRR using 5 sites in the main text (see Fig. 3 and Table III). For instance, by treating the *NYU* site (using the AAL atlas and the SVM classifier) as the target domain, our method using 15 sites as source domains achieves the accuracy of 68.27%, which is lower than that (*i.e.*, 71.88% in Table III in the main text) using 4 source domains. These results are reasonable because the number of subjects in many imaging sites is limited (*e.g.*, < 10 in *SBL* as shown in Table SI), and hence, these samples could not be able to reveal the true data distribution of this site. In such a case, the inclusion of more data from different imaging sites cannot guarantee to boost the classification performance.

C. Results on Unbalanced Dataset

We further evaluate the consistency of our method and each competing method for problems with unbalanced data. In this

TABLE SI
DEMOGRAPHIC INFORMATION OF SUBJECTS FROM THE WHOLE ABIDE DATABASE. THE VALUES ARE DENOTED AS MEAN±STANDARD DEVIATION.
M/F: MALE/FEMALE.

| Site	AAL Atlas				CC200 Atlas			
	ASD		NC		ASD		NC	
	Age	M/F	Age	M/F	Age	M/F	Age	M/F
Caltech	20.43 ± 8.19	7/1	15.74 ± 5.92	10/2	21.08 ± 8.49	6/1	16.27 ± 6.81	12/2
CMU	14.40 ± 0.00	1/0	–	–	14.40 ± 0.00	1/0	–	–
KKI	16.34 ± 8.34	10/2	15.33 ± 5.88	23/2	16.34 ± 8.34	10/2	15.16 ± 5.68	25/2
NYU	17.59 ± 7.84	66/5	16.49 ± 7.68	79/14	17.50 ± 7.76	67/6	16.27 ± 7.65	82/14
MaxMun	19.29 ± 9.14	13/4	17.96 ± 7.25	21/1	18.76 ± 9.15	14/4	17.42 ± 7.23	23/1
Leuven	13.10 ± 4.79	21/4	18.80 ± 9.00	24/8	13.33 ± 4.78	23/4	18.56 ± 8.95	24/7
OHSU	14.72 ± 4.18	9/3	18.27 ± 7.95	10/1	14.72 ± 4.18	9/3	18.27 ± 7.95	10/1
Olin	15.39 ± 7.56	13/1	16.71 ± 7.45	11/0	15.39 ± 7.56	13/1	16.71 ± 7.45	11/0
Pitt	19.99 ± 9.77	13/3	13.79 ± 5.54	10/4	18.93 ± 8.77	17/4	12.87 ± 3.58	15/4
SBL	15.84 ± 3.52	1/2	13.44 ± 4.07	5/0	12.86 ± 3.22	10/4	14.46 ± 5.28	11/0
SDSU	15.42 ± 6.75	9/0	18.35 ± 9.02	15/3	14.88 ± 6.59	10/0	17.47 ± 9.14	13/3
Stanford	15.74 ± 6.58	17/0	20.22 ± 11.95	11/7	15.74 ± 6.58	17/0	19.61 ± 11.92	12/7
Trinity	21.00 ± 9.20	16/5	22.94 ± 11.66	21/0	21.34 ± 9.30	15/5	22.96 ± 11.65	21/0
UCLA	16.27 ± 6.48	28/8	14.65 ± 4.97	31/7	16.11 ± 6.50	27/8	15.12 ± 5.71	32/7
UM	17.05 ± 8.36	43/5	17.35 ± 7.12	56/9	17.27 ± 8.54	40/4	16.81 ± 6.81	52/8
USM	15.77 ± 7.21	30/8	17.34 ± 9.53	21/1	15.77 ± 7.21	30/8	17.34 ± 9.53	21/1
Yale	18.10 ± 7.18	19/2	19.33 ± 9.36	20/6	17.34 ± 6.97	19/2	19.33 ± 9.36	20/6
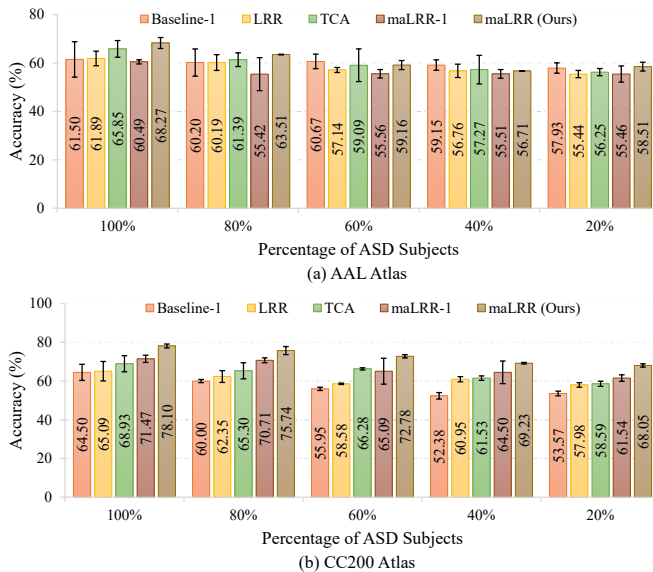
Fig. S2. Performance of five different methods using a certain percentage of ASD subjects and all normal controls from each site. Among all 16 imaging sites, the *NYU* site is treated as the target domain, while the remaining 15 sites as the source domains. (a) Classification results based on data pre-processed by using the AAL atlas. (b) Classification results based on data pre-processed by using the CC200 atlas.

group of experiments, we first randomly select 20%, 40%, 60%, and 80% of ASD subjects (pre-processed by both AAL and CC200 atlases) from each of multiple imaging sites, and then combine these selected ASD subjects and all normal controls (NCs) from this site to construct an unbalanced dataset. Given 16 imaging sites and a specific atlas, we will generate 16 unbalanced datasets, with each dataset corresponding to a specific imaging site. We treat the *NYU* site as the to-be-analyzed target domain and the remaining 15 sites as the source domains. For comparison, we evaluate our method and the competing methods (i.e., Baseline-1, LRR, TCA, and

maLRR-1) on these unbalanced multi-domain datasets, using the same parameter settings as shown in the main text. A 2-fold cross-validation strategy is used to evaluate the performance of all methods. The experimental results are shown in Fig. S2.

From Fig. S2, we can see that, with the decrease of the percentage of ASD subjects in each site, the identification performance becomes slightly worse for all methods, and our maLRR achieves competitive results in most cases. For instance, using 20% ASD subjects in each site, maLRR yields the best classification accuracy of 58.51% and 68.05% with the AAL atlas and the CC200 atlas, respectively, which are higher than the second-best accuracy values of 57.93% (yielded by Baseline-1) and 61.54% (yielded by maLRR-1), respectively. These results suggest that our maLRR generally achieves good performance in ASD diagnosis, even using unbalanced data.

D. Identified Top 10 Brain Connectivity Patterns

We also investigate the top 10 brain connectivity patterns identified by our maLRR method on *NYU* site. It is worth noting that, because the selected brain connectivity patterns are different in each 5-fold cross-validation, we choose the cumulative absolute value [10] as an indicator of the brain connectivity pattern contribution in the classification task. Specifically, we first treat the *NYU* site as the to-be-analyzed target domain and the remaining 4 sites (*i.e.*, *Leuven*, *UCLA*, *UM*, and *USM*) as source domains, and employ the proposed maLRR method to learn the new representation for both source data and target data. Then, we calculate the cumulative absolute value of each connectivity pattern on all subjects (with the new representations) in the *NYU* site, and treat this value as the contribution indicator of each connectivity pattern for the subsequent classification task. We finally show the top 10 identified brain connectivity patterns achieved by our maLRR method in Fig. S3, and list the names of corresponding brain regions in Table SII.
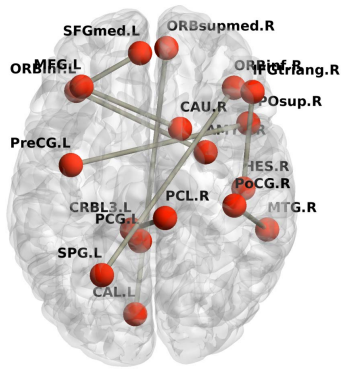
Fig. S3. Top 10 brain connectivity patterns identified by our maLRR method in ASD vs. NC classification on the *NYU* site.

TABLE SII
NAMES OF BRAIN ROIS IN THE TOP TEN CONNECTIVITY PATTERNS IDENTIFIED BY THE PROPOSED METHOD. ROI: REGIONS-OF-INTERSET.

Index of Pairwise ROI	ROI Names
84 & 1	TPOsup.R & PreCG.L
23 & 7	SFGmed.L & MFG.L
72 & 7	CAU.R & MFG.L
80 & 14	HES.R & IFGtriang.R
42 & 15	AMYG.R & ORBinf.L
59 & 16	SPG.L & ORBinf.R
43 & 26	CAL.L & ORBsupmed.R
95 & 35	CRBL3.L & PCG.L
86 & 58	MTG.R & PoCG.R
95 & 70	CRBL3.L & PCL.R

From Fig. S3 and Table SII, we can see that several brain regions have been frequently identified by our method, including *MFG*, *ORBinf* and *CRBL3*. In previous studies [11], [12], these regions are reported to be highly associated with the ASD. In addition, the selected brain regions such as *MTG.R*, *PCG.L*, *SFGmed.L*, and *CAL.L* are also sensitive biomarkers for ASD diagnosis, proven by previous studies [8], [13]–[15]. These results suggest that our method is effective in identifying ASD-related brain regions.

E. Convergence Analysis

We verify the convergence of the proposed maLRR method through experiments on the ABIDE dataset. Although the convergence of ALM has been proved in [6], it is still a challenge to guarantee the convergence with more than two blocks of ALM method. Therefore, we empirically show the convergence of our algorithm, and present the convergence curves of relative absolute error [16] in Fig. S4. From Fig. S4, we can see that the values of the objective function decrease rapidly within thirty iterations and then levels off, which means our algorithm can converge well, especially after 40 iterations.

F. Optimization Algorithm

Algorithm 1 lists the detailed steps for solving the objective function of our maLRR model. Here, we empirically set four parameters μ, ρ, μ_{max} and ε, while tuning the two essential parameters α and β in the experiments. The code has been released, which can be found at http://ibrain.nuaa.edu.cn/.
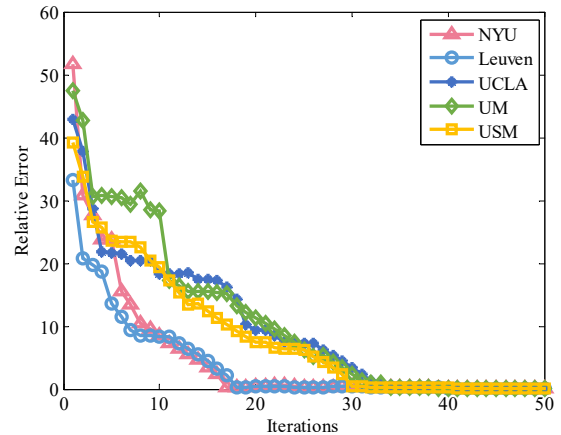

Fig. S4. Convergence of our method on multiple sites settings, where each site serves as the target domain in turn and the remaining sites are selected as the source domains.

REFERENCES

[1] M. A. Di, C. G. Yan, Q. Li, E. Denio, F. X. Castellanos, K. Alaerts, J. S. Anderson, M. Assaf, S. Y. Bookheimer, and M. Dapretto, "The autism brain imaging data exchange: Towards a large-scale evaluation of the intrinsic brain architecture in autism," *Molecular Psychiatry*, vol. 19, no. 6, pp. 659–667, 2014.

[2] C. Cameron, B. Yassine, C. Chu, C. Francois, E. Alan, J. Andras, K. Budhachandra, L. John, Q. Li, and M. Michael, "The neuro bureau preprocessing initiative: Open sharing of preprocessed neuroimaging data and derivatives," *Frontiers in Neuroinformatics*, vol. 7, no. 41, 2013.

[3] N. Tzourio-Mazoyer, B. Landeau, D. Papathanassiou, F. Crivello, O. E-tard, N. Delcroix, B. Mazoyer, and M. Joliot, "Automated anatomical labeling of activations in SPM using a macroscopic anatomical parcellation of the MNI MRI single-subject brain," *NeuroImage*, vol. 15, no. 1, pp. 273–289, 2002.

[4] R. C. Craddock, G. A. James, P. E. Holtzheimer III, X. P. Hu, and H. S. Mayberg, "A whole brain fMRI atlas generated via spatially constrained spectral clustering," *Human Brain Mapping*, vol. 33, no. 8, pp. 1914–1928, 2012.

[5] S. F. Chang, D. T. Lee, D. Liu, and I. Jhuo, "Robust visual domain adaptation with low-rank reconstruction," in *IEEE Conference on Computer Vision and Pattern Recognition*, 2012, pp. 2168–2175.

[6] G. Liu, Z. Lin, S. Yan, J. Sun, Y. Yu, and Y. Ma, "Robust recovery of subspace structures by low-rank representation," *IEEE Transactions on Pattern Analysis and Machine Intelligence*, vol. 35, no. 1, pp. 171–184, 2013.

[7] S. J. Pan, I. W. Tsang, J. T. Kwok, and Q. Yang, "Domain adaptation via transfer component analysis," *IEEE Transactions on Neural Networks*, vol. 22, no. 2, pp. 199–210, 2011.

[8] A. S. Heinsfeld, A. R. Franco, R. C. Craddock, A. Buchweitz, and F. Meneguzzi, "Identification of autism spectrum disorder using deep learning and the ABIDE dataset," *Neuroimage Clinical*, vol. 17, pp. 16–23, 2018.

[9] C. Cameron, S. Sharad, C. Brian, K. Ranjeet, G. Satrajit, C. Yan, Q. Li, L. Daniel, V. Joshua, and B. Randal, "Towards automated analysis of connectomes: The Configurable Pipeline for the Analysis of Connectomes (C-PAC)," *Frontiers in Neuroinformatics*, vol. 7, no. 1, pp. 57–72, 2013.

[10] N. Yahata, J. Morimoto, R. Hashimoto, G. Lisi, K. Shibata, Y. Kawakubo, H. Kuwabara, M. Kuroda, T. Yamada, and F. Megumi, "A small number of abnormal brain connections predicts adult autism spectrum disorder," *Nature Communications*, vol. 7, pp. 1–12, 2016.

[11] R. H. Bennett, K. Somandepalli, A. K. Roy, and A. Di Martino, "The neural correlates of emotional lability in children with autism spectrum disorder," *Brain Connectivity*, vol. 7, no. 5, pp. 281–288, 2017.

[12] Z. Yao, B. Hu, Y. Xie, F. Zheng, G. Liu, X. Chen, and W. Zheng, "Resting-state time-varying analysis reveals aberrant variations of functional connectivity in autism," *Frontiers in Human Neuroscience*, vol. 10, pp. 1–11, 2016.

[13] M. Assaf, C. J. Hyatt, C. G. Wong, M. R. Johnson, R. T. Schultz, T. Hendler, and G. D. Pearlson, "Mentalizing and motivation neural

---

Algorithm 1: Proposed Optimization Algorithm

Input: $\mathbf{X}_T, \mathbf{X}_S, \alpha$ and β;

1 **Initialize:** $\mathbf{Z}_i = \mathbf{0}$, $\mathbf{J} = \mathbf{P} = \mathbf{I}$, $\mathbf{E}_{S_i} = \mathbf{0}$, $\mathbf{E}_{P_i} = \mathbf{0}$, $\mathbf{Y}_{1,i} = \mathbf{0}$, $\mathbf{Y}_{2,i} = \mathbf{0}$, $\mathbf{Y}_{3,i} = \mathbf{0}$, $\mathbf{Y}_4 = \mathbf{0}$, $\mathbf{P}_i = \mathbf{0}$, $\mu = 10^{-5}$, $\rho = 1.2$, $\mu_{max} = 10^7$, $\varepsilon = 10^{-7}$;

2 **while** *not converged* **do**

3   Fix other variables and update $\mathbf{J}$, by solving $\mathbf{J}^{t+1} = \text{argmin}_{\mathbf{J}} \frac{1}{\mu}\|\mathbf{J}\|_* + \frac{1}{2}\|\mathbf{J} - (\mathbf{P}^t + \mathbf{Y}_{4,i}/\mu)\|_F^2$;

4   Fix other variables and update $\mathbf{F}_i$, by solving $\mathbf{F}_i^{t+1} = \text{argmin}_{\mathbf{F}_i} \frac{1}{\mu}\|\mathbf{F}_i\|_* + \frac{1}{2}\|\mathbf{F}_i - (\mathbf{Z}_i^t + \mathbf{Y}_{1,i}/\mu)\|_F^2$;

5   Fix other variables and update $\mathbf{E}_{S_i}$, by solving $\mathbf{E}_{S_i}^{t+1} = \text{argmin}_{\mathbf{E}_{S_i}} \frac{\alpha}{\mu}\|\mathbf{E}_{S_i}\|_1 + \frac{1}{2}\|\mathbf{E}_{S_i} - (\mathbf{P}_i^t\mathbf{X}_{S_i} - \mathbf{P}^t\mathbf{X}_T\mathbf{Z}_i^t + \mathbf{Y}_{2,i}/\mu)\|_F^2$;

6   Fix other variables and update $\mathbf{E}_{P_i}$, by solving $\mathbf{E}_{P_i}^{t+1} = \text{argmin}_{\mathbf{E}_{P_i}} \frac{\beta}{\mu}\|\mathbf{E}_{P_i}\|_1 + \frac{1}{2}\|\mathbf{E}_{P_i} - (\mathbf{P}_i^t - \mathbf{P}^t + \mathbf{Y}_{3,i}/\mu)\|_F^2$;

7   Fix other variables and update $\mathbf{Z}_i$, by solving $\mathbf{Z}_i^{t+1} = [\mathbf{X}_T^T(\mathbf{P}_i^t)^T\mathbf{P}_i^t\mathbf{X}_T + \mathbf{I}]^{-1}[\mathbf{X}_T^T(\mathbf{P}_i^t)^T\mathbf{G}_1 + \mathbf{F}_i^t - \mathbf{Y}_{1,i}/\mu]$;

8   Fix other variables and update $\mathbf{P}_i$, by solving $\mathbf{P}_i^{t+1} = (\mathbf{G}_2\mathbf{X}_{S_i}^T + \mathbf{P}^t + \mathbf{E}_{P_i}^t - \mathbf{Y}_{3,i}/\mu)(\mathbf{X}_{S_i}\mathbf{X}_{S_i}^T + \mathbf{I})^{-1}$;

9   Fix other variables and update $\mathbf{P}$, by solving $\mathbf{P}^{t+1} = [\mathbf{G}_3/\mu + \mathbf{G}_4][\sum_{i=1}^K(\mathbf{X}_T\mathbf{Z}_i^t(\mathbf{Z}_i^t)^T(\mathbf{X}_T)^T + \mathbf{I}) + \mathbf{I}]^{-1}$;

10   then $\mathbf{P} \leftarrow \textbf{orthogonal}(\mathbf{P})$

11   Update the multipliers and parameters by

12     $\mathbf{Y}_{1,i} = \mathbf{Y}_{1,i} + \mu(\mathbf{Z}_i - \mathbf{F}_i)$;

13     $\mathbf{Y}_{2,i} = \mathbf{Y}_{2,i} + \mu(\mathbf{P}_i\mathbf{X}_{S_i} - \mathbf{P}\mathbf{X}_T\mathbf{Z}_i - \mathbf{E}_{S_i})$;

14     $\mathbf{Y}_{3,i} = \mathbf{Y}_{3,i} + \mu(\mathbf{P}_i - \mathbf{P} - \mathbf{E}_{P_i})$;

15     $\mathbf{Y}_4 = \mathbf{Y}_4 + \mu(\mathbf{P} - \mathbf{J})$;

16     $\mu = \min(\mu\rho, \mu_{max})$;

17   Check the convergence conditions

18     $\|\mathbf{P}_i\mathbf{X}_{S_i} - \mathbf{P}\mathbf{X}_T\mathbf{Z}_i - \mathbf{E}_{S_i}\|_\infty < \epsilon$;

19     $\|\mathbf{P}_i - \mathbf{P} - \mathbf{E}_{P_i}\|_\infty < \epsilon$;

20     $\|\mathbf{Z}_i - \mathbf{F}_i\|_\infty < \epsilon$;

21     $\|\mathbf{P} - \mathbf{J}\|_\infty < \epsilon$;

22 **end**

Output: $\mathbf{P}, \mathbf{P}_i, \mathbf{Z}_i, \mathbf{E}_{S_i}, \mathbf{E}_{P_i}$.

---

function during social interactions in autism spectrum disorders," *NeuroImage: Clinical*, vol. 3, pp. 321–331, 2013.

[14] M. Assaf, K. Jagannathan, V. D. Calhoun, L. Miller, M. C. Stevens, R. Sahl, J. G. O'boyle, R. T. Schultz, and G. D. Pearlson, "Abnormal functional connectivity of default mode sub-networks in autism spectrum disorder patients," *NeuroImage*, vol. 53, no. 1, pp. 247–256, 2010.

[15] E. A. von dem Hagen, R. S. Stoyanova, S. Baron-Cohen, and A. J. Calder, "Reduced functional connectivity within and between 'social' resting state networks in autism spectrum conditions," *Social Cognitive and Affective Neuroscience*, vol. 8, no. 6, pp. 694–701, 2012.

[16] Z. Ding, M. Shao, and Y. Fu, "Incomplete multisource transfer learning," *IEEE Transactions on Neural Networks and Learning Systems*, vol. 29, no. 2, pp. 310–323, 2018.

TABLE SIII
PERFORMANCE OF SIX DIFFERENT METHODS IN ASD CLASSIFICATION ON 16 IMAGING SITES FROM ABIDE, WITH DATA PRE-PROCESSED BY USING THE *AAL* ATLAS. EACH OF MULTIPLE DOMAINS IS ALTERNATIVELY USED AS THE TARGET DOMAIN, WHILE THE REMAINING ONES ARE REGARDED AS SOURCE DOMAINS.

Target Site	Method	ACC (%)	SEN (%)	SPE (%)	AUC (%)	BAC (%)	PPV (%)	NPV (%)
Caltech	Baseline-1	56.45±1.95	56.67±3.30	57.14±6.06	60.71±2.53	56.90±1.38	70.00±4.24	56.82±9.64
	LRR	61.81±9.55	72.00±1.31	37.50±5.89	52.50±1.63	54.75±8.60	70.37±5.24	40.38±1.36
	TCA	62.50±3.54	83.33±1.18	31.25±2.65	54.17±1.79	57.29±7.37	65.17±5.74	53.57±5.05
	DAE	60.00±3.43	87.50±5.89	18.75±8.84	44.79±1.47	53.12±1.47	61.81±0.98	50.00±4.16
	maLRR-1	60.20±3.26	61.84±2.75	58.33±2.95	65.52±6.23	60.09±1.00	68.55±7.26	55.00±7.07
	maLRR (Ours)	64.77±5.17	63.14±3.04	66.67±4.71	66.29±1.04	64.90±8.39	76.67±1.89	58.08±2.72
KKI	Baseline-1	59.46±3.82	58.00±2.83	62.50±5.89	59.17±1.65	60.25±4.36	76.32±3.72	41.67±3.93
	LRR	60.81±1.91	64.00±5.66	54.17±1.77	57.33±4.24	59.08±6.01	74.89±5.74	41.45±4.23
	TCA	64.86±3.82	70.00±1.41	54.17±1.68	62.17±2.59	62.08±1.77	76.51±3.45	47.22±3.93
	DAE	63.51±1.91	74.00±1.98	41.67±3.54	55.50±6.84	57.83±7.78	73.85±7.21	42.22±3.14
	maLRR-1	62.16±3.82	62.00±1.80	40.83±2.95	47.00±1.04	51.42±4.83	68.75±2.95	49.23±2.72
	maLRR (Ours)	67.54±1.24	67.31±2.45	66.67±4.71	66.93±1.44	66.99±1.13	86.67±1.89	50.00±2.72
NYU	Baseline-1	61.50±7.33	61.83±1.75	63.38±5.98	69.36±2.55	62.60±5.76	68.54±2.65	57.08±9.27
	LRR	61.89±3.02	70.97±4.56	50.00±1.00	63.23±4.13	60.48±2.78	64.99±1.92	56.92±4.35
	TCA	65.85±3.45	69.89±1.17	60.56±7.97	68.57±4.57	65.23±2.10	69.95±0.60	61.36±6.70
	DAE	63.72±4.31	67.74±9.12	58.45±1.10	65.74±0.58	63.10±0.92	68.36±2.85	58.31±2.39
	maLRR-1	60.49±0.86	66.13±3.88	51.55±1.96	56.14±0.75	53.84±0.54	59.78±0.93	57.46±0.73
	maLRR (Ours)	68.27±2.27	78.52±2.71	54.84±8.87	72.20±5.05	66.68±3.08	69.64±3.34	66.03±0.91
MaxMun	Baseline-1	60.53±1.24	62.50±8.84	58.00±8.49	57.94±2.39	60.25±0.18	65.69±1.39	54.93±2.25
	LRR	62.28±8.68	68.75±2.21	54.00±8.49	64.19±8.93	61.38±6.81	65.23±3.21	60.29±1.46
	TCA	63.16±7.44	85.94±2.21	34.00±1.98	62.94±1.07	59.97±8.79	62.92±6.48	63.07±1.06
	DAE	61.40±2.48	53.12±4.42	72.00±1.31	61.94±8.04	62.56±3.45	71.43±6.73	54.44±1.57
	maLRR-1	64.04±6.20	70.31±1.99	56.00±1.13	63.38±1.08	63.16±4.29	67.08±0.59	61.96±1.20
	maLRR (Ours)	66.67±9.43	68.18±6.43	65.79±1.86	79.19±0.34	66.99±6.09	55.35±1.72	77.94±1.43
Leuven	Baseline-1	59.65±2.48	68.12±1.32	46.00±2.26	57.50±3.01	57.06±4.68	61.52±4.51	56.04±0.68
	LRR	57.88±1.05	59.38±1.33	56.41±1.45	58.55±1.90	57.89±0.62	63.89±3.93	52.27±3.21
	TCA	58.77±1.24	71.88±2.21	42.00±3.11	55.81±0.62	56.94±4.51	62.50±5.89	54.44±1.57
	DAE	60.53±1.24	71.88±4.42	46.00±8.49	65.31±8.04	58.94±2.03	63.12±2.24	56.04±0.68
	maLRR-1	59.65±4.96	73.44±3.15	42.00±5.37	65.19±3.45	57.72±1.03	66.28±1.40	52.78±3.93
	maLRR (Ours)	62.28±6.20	67.31±2.45	50.00±7.07	63.68±1.21	58.65±2.31	82.35±2.50	54.26±3.54
OHSU	Baseline-1	54.37±1.13	53.12±1.33	56.41±1.45	57.41±5.72	54.77±0.62	61.23±3.40	48.53±2.08
	LRR	58.70±3.07	63.64±3.17	54.17±5.89	51.89±1.61	58.90±2.95	56.09±3.17	61.82±2.57
	TCA	60.19±3.26	61.84±2.75	58.33±2.95	65.52±6.23	60.09±1.00	68.55±7.26	55.00±7.07
	DAE	60.87±2.47	54.55±1.86	66.67±1.18	53.41±0.54	60.61±0.54	60.42±2.95	61.82±2.57
	maLRR-1	57.35±1.04	55.56±6.29	56.94±4.52	57.64±2.95	56.25±8.84	55.00±7.07	75.00±3.54
	maLRR (Ours)	64.01±1.48	60.22±0.92	68.97±4.60	73.30±4.32	64.60±1.84	71.84±2.61	56.94±1.19
Olin	Baseline-1	60.00±5.66	77.27±6.43	46.43±5.05	66.56±10.56	61.85±5.74	53.12±4.42	72.22±7.86
	LRR	61.89±3.02	70.97±4.56	50.00±1.00	63.23±4.13	60.48±2.78	64.99±1.92	56.92±4.35
	TCA	66.00±2.83	77.27±6.43	57.14±4.10	68.33±7.35	67.21±1.84	58.89±3.74	76.39±1.96
	DAE	62.00±8.49	72.73±0.95	53.57±8.15	59.74±5.51	63.15±7.58	55.77±8.16	70.83±5.89
	maLRR-1	62.00±1.14	77.27±1.28	50.00±6.10	69.16±2.62	63.64±1.69	54.58±1.20	74.44±2.43
	maLRR (Ours)	70.29±5.12	69.23±2.18	70.91±5.43	74.13±1.48	70.07±3.16	75.56±3.14	67.50±1.06
Pitt	Baseline-1	58.33±2.36	71.43±2.02	46.88±1.32	63.39±1.89	59.15±3.47	53.94±0.86	67.50±3.61
	LRR	60.00±9.43	57.14±4.04	62.50±1.77	67.86±2.53	59.82±1.36	55.00±7.07	67.27±1.80
	TCA	65.00±7.07	85.71±2.02	46.88±1.26	70.98±8.84	66.29±6.63	58.85±6.09	78.41±4.82
	DAE	63.33±4.71	82.14±5.05	46.88±1.33	65.18±0.63	64.51±4.10	57.83±4.64	75.00±1.41
	maLRR-1	61.67±1.18	67.86±2.53	56.25±4.42	66.29±1.54	62.05±1.26	56.58±9.30	69.03±1.81
	maLRR (Ours)	70.00±2.36	78.57±10.10	62.50±5.30	73.21±1.26	70.54±2.15	75.00±3.54	73.33±9.43
SBL	Baseline-1	59.45±1.95	56.67±3.30	57.14±6.06	58.10±2.56	56.90±1.38	70.00±4.24	56.82±1.64
	LRR	60.37±4.31	73.66±1.75	42.96±3.29	58.37±9.85	58.31±7.69	64.38±8.47	54.24±3.38
	TCA	62.20±2.59	59.14±2.13	66.20±2.19	67.84±2.39	62.67±0.31	71.14±6.77	56.36±5.14
	DAE	61.59±2.59	64.52±4.56	57.75±1.20	62.82±3.56	61.13±3.69	67.00±4.76	55.24±1.97
	maLRR-1	64.02±6.04	73.12±7.60	52.11±3.98	66.05±8.13	62.62±5.79	66.58±4.16	59.97±8.67
	maLRR (Ours)	67.66±3.14	63.46±2.49	73.13±10.49	74.09±6.31	68.30±4.00	75.99±6.45	60.34±1.93
SDSU	Baseline-1	59.26±5.24	66.67±7.86	44.44±0.45	66.98±1.40	55.56±3.93	70.49±2.46	40.40±5.71
	LRR	61.11±2.62	75.00±3.93	43.33±1.71	68.21±1.66	54.17±5.89	69.44±3.93	38.89±7.86
	TCA	64.81±2.62	69.44±3.93	55.56±15.71	76.85±0.44	62.50±5.89	76.11±5.50	47.22±3.93
	DAE	62.96±5.24	61.11±7.86	66.67±3.24	67.28±1.09	63.89±3.93	78.46±2.18	46.43±5.05
	maLRR-1	61.11±2.62	63.89±1.18	55.56±1.57	67.59±1.35	59.72±1.96	74.57±3.32	43.65±1.12
	maLRR (Ours)	66.47±2.84	61.36±8.54	73.13±1.05	75.53±7.03	67.25±0.98	75.44±4.73	59.29±1.79
Stanford	Baseline-1	58.57±2.02	74.44±7.86	40.59±1.48	56.05±4.85	57.52±2.31	55.84±1.84	85.71±2.02
	LRR	60.00±4.04	80.56±2.75	38.24±3.74	59.48±0.46	59.40±4.97	59.63±7.18	80.56±2.75
	TCA	64.29±2.02	61.11±1.57	67.65±2.08	63.07±8.78	64.38±2.54	68.45±9.26	62.58±2.42
	DAE	62.86±4.04	69.44±2.50	55.88±3.44	64.38±6.93	62.66±4.97	66.07±12.63	66.15±7.47
	maLRR-1	61.43±1.01	77.78±7.86	44.12±1.25	62.09±0.46	60.95±1.02	59.69±7.81	64.77±1.45
	maLRR (Ours)	67.67±1.42	62.42±7.03	74.52±1.46	74.49±7.49	68.47±2.71	76.96±6.88	60.26±0.37
Trinity	Baseline-1	58.33±1.68	73.81±1.10	42.86±6.73	63.15±2.41	58.33±1.68	56.33±0.47	62.75±5.55
	LRR	60.71±5.05	69.05±3.37	52.38±6.73	64.06±3.69	60.71±5.05	59.25±4.60	62.75±5.55
	TCA	64.29±6.73	76.19±6.73	52.38±20.20	70.18±7.54	64.29±6.73	62.42±8.14	68.33±2.36
	DAE	63.10±8.42	69.05±3.37	57.14±1.35	68.48±9.94	63.10±8.42	62.09±8.61	64.41±7.90
	maLRR-1	61.90±3.37	54.76±2.36	69.05±1.68	64.17±3.53	61.90±3.37	64.58±2.95	61.67±7.07
	maLRR (Ours)	66.59±9.32	70.91±1.54	52.27±3.21	68.56±3.45	61.59±9.32	59.42±6.89	65.28±1.38
UCLA	Baseline-1	60.14±0.96	69.74±3.91	50.00±3.28	64.14±2.42	59.87±0.10	61.79±6.89	72.44±2.32
	LRR	62.16±1.91	86.84±1.49	36.11±1.96	64.36±2.12	61.48±2.38	59.31±3.38	77.78±1.57
	TCA	66.89±4.78	80.26±5.58	52.78±3.93	67.32±6.31	66.52±4.76	64.18±3.51	71.79±7.25
	DAE	67.57±3.82	81.58±3.72	52.78±3.93	71.82±0.05	67.18±3.82	64.58±2.95	73.08±5.44
	maLRR-1	64.19±0.96	77.63±1.86	50.00±0.75	67.36±6.36	63.82±0.93	62.10±0.56	67.95±1.81
	maLRR (Ours)	68.92±5.73	71.05±3.72	66.67±7.86	71.78±0.62	68.86±5.79	69.34±6.14	68.46±5.31
UM	Baseline-1	59.73±0.63	70.77±3.70	44.79±4.86	60.48±0.97	57.78±5.81	66.90±1.06	61.39±1.42
	LRR	62.39±3.13	69.23±6.53	53.12±1.47	63.24±3.58	61.18±2.53	66.62±1.40	56.29±4.57
	TCA	65.93±4.38	70.00±1.20	60.42±5.89	69.95±0.61	65.21±3.04	70.50±0.47	60.61±7.42
	DAE	66.37±3.75	69.23±1.31	62.50±3.84	71.15±1.09	65.87±2.11	71.53±0.98	60.89±7.02
	maLRR-1	64.60±6.26	71.54±5.79	55.21±1.47	65.54±6.84	63.37±5.63	68.23±3.68	59.46±9.05
	maLRR (Ours)	69.05±3.37	70.98±1.90	66.67±1.68	73.41±7.04	68.82±0.64	75.11±5.74	64.90±1.36
USM	Baseline-1	61.67±2.36	70.45±3.21	56.58±5.58	67.94±1.52	63.52±1.18	48.53±2.08	76.79±0.18
	LRR	64.17±5.89	68.18±6.43	61.84±5.58	71.53±2.71	65.01±6.01	50.92±6.01	76.99±5.17
	TCA	65.00±2.36	75.00±9.64	59.21±1.86	74.22±10.40	67.11±3.89	51.47±2.08	80.64±5.62
	DAE	65.83±3.54	70.45±3.21	63.16±3.72	70.16±4.65	66.81±3.47	52.59±3.66	78.66±2.81
	maLRR-1	62.50±1.18	61.36±9.64	63.16±3.72	65.97±1.27	62.26±2.96	49.00±1.41	74.05±3.70
	maLRR (Ours)	68.33±1.18	68.18±6.43	68.42±2.33	79.43±0.68	68.30±7.95	58.53±1.62	78.46±2.18
Yale	Baseline-1	60.64±4.51	58.08±1.36	66.19±2.69	66.76±1.20	62.13±6.67	76.70±2.10	53.86±2.39
	LRR	61.98±5.18	63.40±2.96	60.42±2.65	65.84±6.15	61.91±1.57	69.77±5.54	58.33±1.18
	TCA	64.89±1.50	64.23±8.16	70.48±6.73	75.46±0.26	67.35±0.71	76.08±6.83	66.81±1.77
	DAE	67.02±4.51	75.77±2.45	60.95±2.02	72.62±3.76	68.36±2.14	71.99±1.26	71.11±7.86
	maLRR-1	62.77±4.51	63.46±1.90	61.90±3.37	68.41±1.02	62.68±7.32	70.93±1.46	57.60±0.65
	maLRR (Ours)	70.38±1.14	76.92±2.18	61.82±2.57	73.81±1.64	69.37±9.59	70.83±5.89	72.02±1.94

TABLE SIV

PERFORMANCE OF SIX DIFFERENT METHODS IN ASD CLASSIFICATION ON 16 IMAGING SITES FROM ABIDE, WITH DATA PRE-PROCESSED BY USING THE *CC200* ATLAS. EACH OF MULTIPLE DOMAINS IS ALTERNATIVELY USED AS THE TARGET DOMAIN, WHILE THE REMAINING ONES ARE REGARDED AS SOURCE DOMAINS.

Target Site	Method	ACC (%)	SEN (%)	SPE (%)	AUC (%)	BAC (%)	PPV (%)	NPV (%)
Caltech	Baseline-1	57.73±1.74	57.14±0.61	50.00±0.71	75.10±2.19	53.57±1.05	75.00±1.21	55.12±1.99
	LRR	61.90±6.73	65.00±2.53	53.71±3.03	54.08±2.89	55.36±2.53	70.57±3.04	45.00±3.07
	TCA	69.05±3.37	65.71±1.01	55.71±3.30	67.35±1.87	60.71±1.01	73.50±7.18	53.57±5.05
	DAE	66.67±6.73	71.43±5.10	57.14±5.10	73.98±6.49	64.29±5.05	76.79±2.53	50.79±8.98
	maLRR-1	59.52±3.37	60.71±5.05	57.14±4.81	60.71±2.27	58.93±2.53	73.86±1.61	42.22±3.14
	maLRR (Ours)	74.12±1.54	71.71±4.65	76.80±1.10	82.46±0.73	74.25±1.88	78.33±1.01	70.45±4.12
KKI	Baseline-1	58.97±7.25	62.96±3.66	50.00±5.93	66.20±1.11	56.48±1.13	69.74±1.58	52.14±1.10
	LRR	61.54±3.63	66.67±3.14	52.33±1.01	69.29±2.25	58.33±1.36	60.44±1.68	53.65±1.22
	TCA	66.67±3.63	74.07±2.95	50.00±5.89	67.90±2.05	62.04±1.90	71.34±1.81	47.50±1.76
	DAE	65.38±5.44	57.41±2.62	83.33±9.79	83.18±1.09	70.37±7.20	88.73±7.63	46.43±5.05
	maLRR-1	56.58±0.93	55.22±1.28	58.33±5.89	72.25±2.47	56.78±2.31	62.14±2.53	51.41±2.09
	maLRR (Ours)	73.33±9.43	86.36±6.43	65.79±18.61	86.84±1.01	76.08±6.09	60.93±11.74	89.57±1.89
NYU	Baseline-1	64.50±4.18	77.60±2.43	47.26±4.17	79.27±1.22	62.43±0.87	68.80±1.21	65.90±0.89
	LRR	65.09±5.02	73.96±2.95	53.42±5.04	79.68±0.65	63.69±1.05	73.35±1.85	65.66±9.29
	TCA	68.93±4.18	65.10±1.69	73.97±2.13	78.49±1.04	69.54±2.18	78.80±1.08	62.62±4.99
	DAE	66.57±3.77	77.08±2.10	52.74±4.72	72.27±4.75	64.91±4.36	68.32±4.01	63.43±3.85
	maLRR-1	71.47±1.86	91.67±1.18	57.14±4.04	79.29±1.92	74.40±1.43	66.67±2.36	92.86±1.01
	maLRR (Ours)	78.10±1.02	75.00±3.84	82.28±4.34	86.30±3.53	78.64±0.25	85.22±5.61	71.88±5.37
MaxMum	Baseline-1	57.14±1.35	54.17±4.13	61.11±2.36	58.80±3.27	57.64±2.84	63.33±4.71	55.21±1.62
	LRR	60.71±5.05	66.67±1.18	52.78±2.93	63.43±1.95	59.72±3.93	65.15±2.14	55.00±7.07
	TCA	61.90±3.37	62.50±1.76	61.11±1.57	62.96±4.58	61.81±0.98	68.63±2.77	56.00±5.66
	DAE	67.75±2.09	63.02±1.98	73.97±2.13	78.18±0.61	68.50±0.71	78.30±1.01	61.59±6.46
	maLRR-1	63.10±1.68	60.42±2.06	66.67±2.36	63.43±3.93	63.54±1.47	72.62±3.42	56.79±4.55
	maLRR (Ours)	71.15±2.72	73.33±0.21	68.18±6.43	81.67±1.71	70.76±3.21	75.95±3.70	65.15±2.14
Leuven	Baseline-1	56.90±2.44	62.26±6.84	47.78±2.62	65.41±0.42	55.02±2.11	56.63±1.15	58.48±7.29
	LRR	61.21±3.66	74.19±3.65	46.30±3.41	70.01±9.80	60.24±1.22	62.42±3.96	77.14±3.23
	TCA	66.38±3.66	75.16±6.84	53.33±1.57	74.61±3.29	64.25±4.44	62.37±3.89	70.00±1.41
	DAE	64.65±6.10	67.10±4.56	58.89±7.86	69.06±4.56	62.99±6.21	62.10±4.26	72.14±1.11
	maLRR-1	62.07±7.31	65.48±1.60	55.19±2.62	65.47±1.50	60.33±6.67	60.00±3.54	72.78±2.44
	maLRR (Ours)	70.71±1.01	67.50±1.06	74.45±1.43	74.26±4.21	70.98±1.88	76.20±1.94	66.97±3.20
OHSU	Baseline-1	55.77±8.16	71.67±1.79	48.57±2.20	65.48±8.42	60.12±4.21	50.51±7.14	77.50±1.68
	LRR	63.04±3.07	72.73±2.57	54.17±2.95	73.48±5.36	63.45±1.87	61.11±7.86	72.14±1.11
	TCA	67.39±9.22	75.45±6.43	61.67±1.17	79.92±3.75	68.56±9.11	60.13±6.47	70.00±1.41
	DAE	65.22±1.30	50.00±3.21	79.17±5.89	78.41±0.54	64.58±1.12	66.36±9.00	65.28±3.75
	maLRR-1	60.87±6.15	77.27±3.14	45.83±4.25	78.03±1.79	61.55±4.55	59.52±1.01	72.14±2.53
	maLRR (Ours)	76.90±4.38	75.00±8.84	79.47±1.54	85.94±4.59	77.23±3.65	82.74±0.34	71.11±7.36
Olin	Baseline-1	54.00±1.41	59.09±3.21	50.00±5.05	62.01±2.43	54.55±0.92	54.76±1.68	56.58±0.93
	LRR	62.00±0.85	68.18±4.50	57.14±5.05	75.97±1.75	62.66±2.75	65.00±2.12	72.50±2.48
	TCA	64.00±1.70	65.45±0.64	69.29±3.54	76.62±0.92	67.37±1.45	57.25±1.33	75.00±0.71
	DAE	64.00±1.13	70.91±1.29	62.86±3.03	78.57±0.92	66.88±0.87	57.14±1.01	70.91±1.29
	maLRR-1	63.46±1.90	65.00±2.12	64.29±5.05	80.48±2.09	64.64±1.47	72.22±3.93	68.33±2.36
	maLRR (Ours)	67.31±2.45	73.33±0.94	64.29±5.05	79.29±1.92	68.81±2.05	72.22±3.93	72.22±0.79
Pitt	Baseline-1	58.75±0.88	66.84±1.86	53.33±3.37	71.68±2.48	60.09±2.53	55.43±1.69	85.29±2.08
	LRR	62.50±1.06	78.95±0.74	47.62±2.69	69.17±0.53	63.28±1.75	59.14±1.64	70.18±4.96
	TCA	67.50±3.53	81.58±1.16	54.76±3.37	78.32±6.91	68.17±3.90	61.92±1.48	77.60±4.92
	DAE	68.75±5.30	86.84±1.86	52.38±0.67	77.57±5.85	69.61±5.94	62.10±1.74	85.29±2.08
	maLRR-1	59.08±5.77	58.79±1.79	58.33±5.89	74.77±2.66	58.56±2.05	63.33±2.36	53.08±1.85
	maLRR (Ours)	72.81±2.68	73.89±5.50	71.82±1.16	81.62±5.71	72.85±4.54	70.71±1.00	75.00±3.07
SBL	Baseline-1	54.76±1.01	54.17±4.13	55.56±3.14	60.19±2.62	54.86±4.91	61.25±1.77	51.88±1.49
	LRR	52.24±0.86	56.67±3.30	50.00±1.01	65.48±2.42	53.33±1.15	45.00±0.71	62.50±1.77
	TCA	54.76±3.37	60.83±1.76	43.33±3.14	60.19±3.93	52.08±1.87	59.60±5.71	41.67±1.18
	DAE	64.10±3.62	56.67±3.30	71.43±2.02	66.67±2.67	64.05±1.40	61.90±1.73	70.00±1.41
	maLRR-1	58.95±1.49	62.36±2.29	50.00±4.71	70.97±2.30	56.18±1.21	67.23±1.20	43.33±1.18
	maLRR (Ours)	67.63±1.31	65.00±2.12	71.43±4.04	69.05±3.37	68.21±1.60	75.00±3.54	72.50±3.54
SDSU	Baseline-1	63.46±2.72	67.50±0.62	45.00±0.71	67.19±1.02	56.25±3.54	65.15±2.14	55.00±3.07
	LRR	63.75±1.24	82.11±1.12	48.10±1.35	73.56±1.15	65.10±1.23	57.47±0.83	83.33±2.36
	TCA	67.31±2.72	84.38±4.42	40.00±1.41	71.56±3.98	62.19±4.86	69.44±3.93	61.25±1.77
	DAE	68.75±5.30	86.84±1.86	52.38±0.67	77.57±5.85	69.61±5.94	62.10±1.74	85.29±2.08
	maLRR-1	65.38±1.41	77.50±5.44	50.00±1.14	68.12±1.15	58.75±0.71	66.82±4.50	58.33±1.18
	maLRR (Ours)	73.08±5.44	75.00±3.28	70.00±1.41	77.50±1.06	72.50±7.07	80.36±7.58	63.33±4.71
Stanford	Baseline-1	59.72±1.96	55.26±3.35	64.71±3.33	65.33±3.50	59.98±0.11	67.50±1.06	58.60±0.71
	LRR	63.89±3.93	63.16±2.23	64.71±3.28	70.74±1.12	63.93±5.47	70.91±5.43	61.82±2.57
	TCA	66.67±7.86	78.95±3.25	52.94±1.66	67.03±5.91	65.94±3.32	65.71±2.08	68.48±6.86
	DAE	69.44±3.93	63.16±2.23	76.47±1.64	74.92±5.25	69.81±2.85	76.62±7.35	66.67±5.43
	maLRR-1	65.28±1.96	73.68±3.72	55.88±4.58	77.86±1.09	64.78±4.27	70.60±1.87	80.00±2.83
	maLRR (Ours)	75.39±2.85	80.00±2.28	70.14±1.08	77.92±1.77	75.07±3.74	75.00±2.53	81.81±2.71
Trinity	Baseline-1	59.76±1.72	80.95±2.69	37.50±2.48	64.88±2.10	59.23±1.09	57.92±1.65	78.95±2.98
	LRR	62.20±1.72	76.19±6.73	47.50±1.61	62.98±2.86	61.85±1.94	60.56±2.74	65.69±1.39
	TCA	67.07±5.17	59.52±1.68	75.00±2.83	70.12±1.72	67.26±5.72	76.70±2.01	64.02±0.97
	DAE	70.73±3.45	78.57±1.01	62.50±3.54	75.95±1.44	70.54±3.28	68.71±0.74	74.21±4.19
	maLRR-1	64.63±5.17	76.19±6.73	52.50±1.77	64.76±5.39	64.35±5.47	63.40±6.76	67.54±1.24
	maLRR (Ours)	75.48±7.74	80.00±2.28	70.00±1.41	78.59±1.34	75.00±7.07	74.17±1.18	83.33±2.36
UCLA	Baseline-1	65.54±0.96	61.54±2.54	70.00±2.63	73.48±1.24	65.77±0.44	72.77±1.16	63.86±7.59
	LRR	63.51±5.73	83.33±1.23	41.43±2.02	71.58±5.28	62.38±5.34	61.17±2.81	71.18±1.58
	TCA	69.59±2.87	71.79±2.90	67.14±3.84	76.74±2.02	69.47±4.69	77.03±1.96	72.91±1.34
	DAE	68.92±3.82	75.64±5.44	61.43±1.41	77.88±4.97	68.53±4.35	69.13±6.44	69.34±0.15
	maLRR-1	66.22±1.91	67.95±3.45	64.29±3.44	73.96±1.92	66.12±0.05	72.06±1.26	70.42±1.69
	maLRR (Ours)	75.58±4.76	71.84±2.61	79.74±1.29	82.47±1.14	75.79±5.17	80.59±4.77	71.66±1.51
UM	Baseline-1	60.58±1.36	59.17±3.65	62.50±4.66	70.98±1.45	60.83±5.04	76.55±2.03	55.16±5.57
	LRR	64.90±6.12	77.50±2.95	47.73±5.46	75.51±0.29	62.62±1.59	72.30±1.96	69.69±1.58
	TCA	67.31±2.72	53.33±4.71	86.36±2.63	73.96±1.90	69.85±2.36	84.17±1.18	57.63±2.47
	DAE	69.23±1.22	85.83±1.76	46.59±5.30	80.38±6.59	66.21±1.77	72.94±1.89	74.91±7.20
	maLRR-1	63.46±2.72	67.50±2.48	57.95±4.01	66.69±8.38	62.73±7.71	72.76±1.50	57.49±2.27
	maLRR (Ours)	76.92±1.47	68.33±2.36	88.64±3.21	82.20±1.39	78.48±0.43	89.20±2.41	67.26±0.84
USM	Baseline-1	65.00±4.71	70.45±9.64	61.84±1.86	74.40±1.66	66.15±5.75	51.56±4.64	78.48±6.06
	LRR	63.94±6.12	52.50±2.71	79.55±2.25	76.99±5.97	66.02±0.23	81.90±1.28	56.72±7.78
	TCA	66.25±2.72	56.67±2.12	79.55±2.25	77.80±7.12	68.11±0.64	82.74±1.39	58.38±5.43
	DAE	70.00±2.36	54.55±3.21	78.95±2.23	82.72±1.10	66.75±4.91	66.31±1.62	76.67±8.61
	maLRR-1	68.33±2.43	59.09±6.43	73.68±1.86	77.27±4.72	66.39±3.09	59.43±1.58	75.47±1.80
	maLRR (Ours)	76.67±3.43	86.36±6.43	71.05±1.61	86.84±1.21	78.71±6.09	65.28±1.38	90.28±1.96
Yale	Baseline-1	60.64±4.51	67.31±4.08	52.38±4.04	77.75±2.46	59.84±0.19	66.20±7.39	67.42±2.25
	LRR	62.50±2.72	70.00±4.01	52.27±6.11	79.28±5.04	61.14±1.05	76.09±2.33	67.27±1.80
	TCA	64.90±4.76	78.33±9.43	46.59±2.41	66.76±8.49	62.46±7.34	67.54±7.56	60.66±2.21
	DAE	68.09±1.50	63.46±3.54	73.81±1.01	83.42±5.57	68.64±1.26	74.05±3.70	66.93±2.18
	maLRR-1	63.83±3.01	68.08±2.72	71.43±1.01	81.43±1.53	69.75±3.69	70.80±2.41	62.86±2.10
	maLRR (Ours)	74.64±1.13	73.08±5.44	76.82±1.86	84.93±0.94	74.95±1.20	80.07±1.53	69.32±2.04